BEAM DYNAMICS FOR A PHOTOINJECTED ENERGY RECOVERY LINAC AT THE NSLS*

J.B. Murphy, I. Ben-Zvi, N. Towne, J.M. Wang, X.J. Wang, J.H. Wu, V. Yakimenko
NSLS, BNL, Upton, NY 11973

Abstract

The Photoinjected Energy Recovery Linac (PERL) design study at the NSLS is considering the feasibility of a new synchrotron light source based on a 3-7 GeV energy recovering superconducting linac initiated by a photo-injected RF gun [1]. To be a competitive light source the photoinjector must provide high brightness electron beams with a normalized transverse emittance of 0.5-1 mm-mrad and a bunch charge per of 0.15-0.45 nC at a rep rate of 0.43-1.3 GHz. We provide a first pass assessment of some of the beam dynamics issues that are critical to preserving the high brightness beams.

1 INTRODUCTION

As presently conceived the NSLS PERL consists of a 3 GeV superconducting linac, based on the 1.3 GHz TESLA design, together with a return leg lattice as shown in Figure 1. Parameters for the PERL source under study at the NSLS are given in Table 1.

Table 1: NSLS PERL Specifications

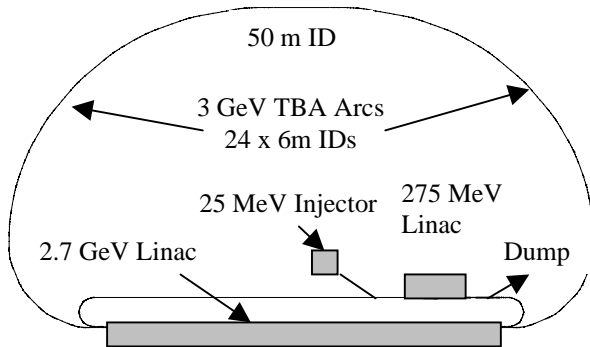| Parameter [Units]	Value
Energy, E [GeV]	3-7
Normalized Emittance, ε_N [mm-mrad]	0.5-1
Bunch Length in IDs, σ_t [fs]	100-400
Normalized Energy Spread, σ_e [%]	<0.1
Average Current, I [ma]	100-200
Charge/Bunch, Q [nC]	0.075-0.45
Rep Rate, f [GHz]	1.3-0.43
Brightness [ph/sec/0.1%BW/mm^{2}mrad^2]	>10^{21}

Figure 1: 3 GeV PERL Schematic Layout

The goal of a PERL based light source is to merge the high brightness electron beams made possible by photo-cathode based RF guns together with superconducting linac technology to produce a new generation of synchrotron light sources with transverse emittances of a few angstroms, pulse lengths on the order of 100 fs, while still maintaining 100+ ma average current. It is of interest to compare the electron beam parameters of the PERL with those of the LCLS project: the normalized emittance is virtually the same, each PERL bunch contains roughly 1/6 of the LCLS charge and it is 50 % longer, however the bunch rep rate in PERL is a factor of 10^7 higher for the 100-200 ma average current

2 INCOHERENT RADIATION EFFECTS

2.1 Radiated Power

The incoherent synchrotron radiation power in the bending magnets (BM) & insertion devices (ID) is,

$$P[KW] = 1.27\ E^2[GeV]\ I[A]\begin{cases} B^2[T]\ L_{BM}[m] \\ B^2[T]\ L_{ID}[m]/2 \end{cases}. \quad (1)$$

For 2π of BMs with B = 1.43 T, ρ = 7 m, this amounts to 205 KW for 0.2 A at 3 GeV. The power in the IDs is 30 KW for λ_u = 3.3 cm, B = 0.47 T & N_u =150 x 24.

2.2 Energy Spread

Due to quantum fluctuation, incoherent synchrotron radiation in the BMs & IDs gives rise to a normalized energy spread in a single pass [2,3]:

$$\sigma_e = \sqrt{\frac{55 r_e c \lambda_c}{24\sqrt{3}}\frac{\gamma^5}{\rho_{BM}^3}\frac{2\pi\rho_{BM}}{c\beta}\left(1+\frac{4}{3\pi}\left(\frac{\rho_{BM}}{\rho_{ID}}\right)^3\frac{N_u\lambda_u}{2\pi\rho_{BM}}\right)}. \quad (2)$$

For 3 GeV and ρ = 7 m, σ_e^{BM} = 3.6×10^{-5}; taking λ_u = 3.3 cm, B = 0.47 T, & N_u = 150 x 24, only increases the energy spread by 2%. It should be noted that the contribution of the small arcs at 300 MeV are negligible.

2.3 Incoherent Emittance Growth

If the photons are emitted in a region of the lattice where there is dispersion there is a contribution to the horizontal emittance of the electron beam [2],

$$\Delta\varepsilon_x = \frac{\sigma_{e,BM}^2}{L_{BM}}\left[\int_{BM} Hds + \frac{4}{3\pi}\left(\frac{\rho_{BM}}{\rho_{ID}}\right)^3\int_{ID} Hds\right], \quad (3)$$

where $H(s) \equiv \gamma\eta^2 + 2\alpha\eta\eta' + \beta\eta'^2$. The second term due to the IDs is usually negligible as the IDs are in zero dispersion locations and their "self dispersion" is small. Just as in a ring, one must keep $\int_{BM} Hds$ small by using many cells in the arcs. Note the very rapid scaling of the energy spread with electron energy, $\sigma_e^2 \propto \gamma^5$.

3 LATTICE & BUNCH COMPRESSION

The complete return leg is split into two loops, of 0.3 and 3 GeV, so that the input and output energy ratio of each linac is roughly 10 thereby simplifying the focusing in the linacs [4]. The 0.3 and 3 GeV arcs have 8 & 24 triple bend achromat cells respectively to yield a small contribution to the incoherent emittance growth in equation (3). Tuning of the dispersion in the center dipole of the TBA cells provides a variable R_{56}, which is coupled with an energy chirp in the linac sections, to yield longitudinal bunch compression by a factor of 30. Work is in progress with PARMELA to obtain an accurate distribution function for a beam from an L-band photoinjector and a 25 MeV booster linac. For the present calculations the RMS longitudinal emittance of the 25 MeV beam is assumed to be 3 ps x 0.1% and bi-Gaussian.

Bunch compression is done in two stages: from 3 ps → 400 fs in the 275 MeV linac and small arc and from 400 fs → 100 fs in the 2.7 GeV linac and the first half of the large arc. A third harmonic cavity (3.9 GHz) is used to remove RF curvature in the 275 MeV linac and sextupoles are used to compensate the T_{566} elements in the arcs. To prepare the beam for energy recovery, the compression cycle is reversed in the second half of the large arc where the bunch is stretched to 400 fs; and finally back to 3 ps in the return through the 300 MeV loop to 25 MeV. The details of the final stage of energy recovery and the beam dump are under study.

4 LONGITUDINAL WAKEFIELDS

Since one of the primary goals of the PERL source is to produce short electron bunches, ~ 100 fs, wakefields can enhance the energy spread of the electron beam and also gives rise to a coherent power loss proportional to the charge per bunch squared. Table 2 lists the longitudinal Green's function wakes considered so far in our analysis.

In Table 3 and Figure 2 we give analytic & numerical results for the power/length and normalized energy spread/length generated by these wakes, each considered independently, and for Gaussian bunches with 0.15 nC spaced at 1.3 GHz. Work is in progress to include all of the wakefields simultaneously into the ELEGANT tracking code so that cancellation or enhancement among the wakes can be assessed and the effects on bunch compression can be analyzed.

Table 2: Longitudinal Green's Function Wakefields

Model	Green's Function Wakefields
Resistive Wall [5]	$\dfrac{c}{4\pi a s^{3/2}}\sqrt{\dfrac{Z_0}{\pi\sigma_c}}H(s)$
Multi-cell SC Linac [6]	$-\dfrac{cZ_0}{\pi a^2}\left(1.165\mathrm{Exp}[-\sqrt{s/s_0}]-0.165\right)H(s)$
Coherent Syn. Rad.[7]	$\dfrac{1}{4\pi\varepsilon_0}\dfrac{2}{3^{4/3}\rho^{2/3}s^{4/3}}H(-s)$

4.1 Resistive Wall

As presently envisioned, the bunch in the 3 GeV arc varies from 0.4 ↔ 0.1 ps, so for IDs with a copper chamber and a = 5 mm, 74 ≤ P/L ≤ 592 w/m and 0.13 ≤ σ_E / L ≤ 3.2 x 10^{-6}/m. As seen from Table 3, the results for smaller gap IDs can be obtained by a simple scaling by 1/a.

Table 3: Power/Length and Energy Spread/Length

Model	P/L [w/m]	σ_E / L [1/m]
Resistive Wall [5]	$\dfrac{cf_{rep}\,N^2\,q^2\Gamma\left[\frac{3}{4}\right]}{4\pi^2 a\sigma^{3/2}}\sqrt{\dfrac{Z_0}{2\sigma_c}}$	$\dfrac{0.023\,N\,q^2}{acm\gamma\sigma^{3/2}}\sqrt{\dfrac{Z_0}{\sigma_c}}$
Coherent Syn.Rad.[7]	$\dfrac{f_{rep}N^2q^2\Gamma\left[\frac{5}{6}\right]}{4\pi^{3/2}6^{1/3}\varepsilon_0\rho^{2/3}\sigma^{4/3}}$	$\dfrac{0.246\,N\,r_e}{\gamma\rho^{2/3}\sigma^{4/3}}$

4.2 Multi-Cell Linac

In the SC linac the electron bunches are 400 fs long, yielding P/L = 400 w/m and σ_E / L = 4x10^{-7}/m. The impact of this heat on the cryogenic system of the 150 meter SC linac is under consideration.
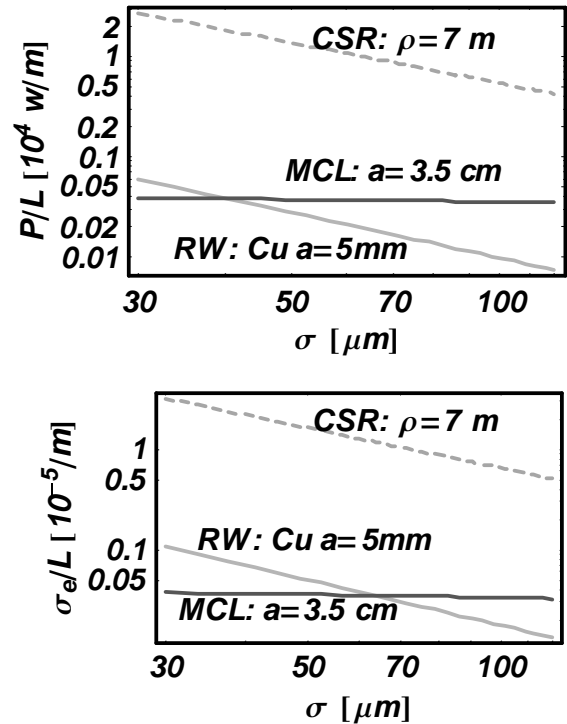

Figure 2: Power/Length and Energy Spread/Length vs. Bunch Length for CSR, Resistive Wall & Multi-Cell Linac Wakefields Assuming Gaussian Bunches

4.3 Coherent Synchrotron Radiation (CSR)

As is evident from Figure 2, CSR has the largest effect on the beam: 4.2 ≤ P/L ≤ 27 KW/m and 0.5 ≤ σ_E / L ≤ 3.2 x 10^{-5}/m. This implies that in $2\pi\rho$, with ρ = 7 m, the coherent synchrotron radiation power is in the range: 0.19 ≤ P/L ≤ 1.2 MW, depending on the compression scheme

in the arc. Thus the CSR power can be significantly greater than the incoherent power discussed in equation (1) and some provision for dealing with the copious amounts of infrared radiation will have to be made. From the work in [7] on shielding of CSR, one can estimate the height of a pair of parallel plates above the electron beam, ±h, to reduce the CSR power by a factor of 10,

$$h \approx \sigma^{2/3}\rho^{1/3}/0.8^{2/3} . \qquad (4)$$

For $\sigma = 120$ μm and $\rho = 7$ m this gives h = 5.4 mm and for $\sigma = 30$ μm we have h = 2.1 mm; the first case is possible, but the second case produces too small of a gap.

What's missing from the simple formulas in Table 3 is the fact that the bunch length in the PERL arcs is changing and in fact the head and tail of the bunch are interchanged. In the first half of the 3 GeV arc the tail of the bunch loses energy and the head gains thus initiating an energy spread. Following the interchange of the head and tail, the "new" tail of the bunch loses energy and the head gains in the second half of the 3 GeV arc. Using the model of the CSR wake in the ELEGANT code [8] we have shown that the net energy spread induced by CSR can be significantly reduced by this interchange of the head and tail [9]. The "coherent" nature of the wake induced energy spread can be used to produce a cancellation effect.

By its very nature, an energy recovery linac using a single linac structure requires the electron beam to be bent by at least 2π to decelerate the beam. As such, CSR induced emittance growth is a serious concern and it has been analyzed for PERL [9] using the ELEGANT code. As discussed in references [10,11], due to its "coherent nature", it is possible to obtain some cancellation of emittance growth in succeeding dipole magnets by a judicious use of –I transforms. By choosing a horizontal betatron phase advance of $(2n+1)\pi$ between the successive TBA cells in the 3 GeV arc, the ELEGANT simulation indicates it is possible to nearly cancel the CSR emittance growth for 0.15 nC in a bunch that is compressed to 100 fs RMS [9].

4.4 Surface Roughness Wake

The surface roughness wake, which has been the subject of much discussion in relation to the LCLS project [12], is under consideration. With 1/6 less charge per bunch and 50% longer bunches than LCLS, PERL should be fine assuming LCLS is possible and the ID gaps are not assumed to be less than the 5mm full gap.

5 TRANSVERSE WAKEFIELDS

5.1 Multi-Turn Beam Breakup

The TDBBU code [13] is being used to assess the current limit imposed by the interaction of the recirculating electron beam with a set of 10 HOMs in the TESLA style SC linac. Various focusing schemes in the 2.7 GeV linac (constant quadrupole gradient, etc.) and the return leg lattice are being explored to maximize the circulating current. Preliminary analysis indicates that threshold currents in excess of 200 ma are possible in the 0.3-3 GeV loop. Enhancements to the TDBBU code are underway to consider both the 0.3 & 3 GeV loops simultaneously [14]. Also a "single energy loop" design for PERL is under consideration.

6 BEAM STABILITY

At 3 GeV the uncorrupted geometrical emittance is 0.8-1.7 Å which together with $\beta = 2$ m yields a beam size of $\sigma \sim 13$-20 μm, with even lesser values if small gap IDs are used. The challenge of building feedback systems to stabilize the orbit position to the desired micron to sub micron levels at all source points in a single pass machine with a laser driven photoinjector is formidable.

7 CONCLUDING REMARKS & OUTLOOK

We presented a status report of the preliminary beam dynamics analysis of a photoinjected energy recovery linac under study at the NSLS. We conclude that the PERL concept, while presenting some real technical challenges, has great promise as a future high brightness, sub-picosecond light source.

8 ACKNOWLEDGEMENTS

9 REFERENCES

[1] I. Ben-Zvi, et. al, these proceedings (2001).
[2] M. Sands, SLAC-121 (1972).
[3] E.L. Saldin, et. al., NIM A381, 545 (1996).
[4] V. Yakimenko, et. al, these proceedings (2001).
[5] O. Henry & O. Napoly, Part. Acc., p. 235 (1991).
[6] R. Brinkmann, et. al., Proc. EPAC 2000, p. 2028 (2000).
[7] J.B. Murphy, S. Krinsky & R.L. Gluckstern, Part. Acc., p. 9 (1997).
[8] M. Borland, APS LS-287 (2000).
[9] J.H. Wu, et. al, these proceedings (2001).
[10] LCLS Design Study Group, SLAC-R-521 (1998).
[11] D. Douglas, JLAB-TN-98-012 (1998).
[12] G. Stupakov, SLAC-PUB-8743 (2000).
[13] G.A. Krafft and J.J. Bisognano, Proc. IEEE PAC, p. 1356 (1987).
[14] N. Towne, private communication (2001).